



Matjaž Mikoš · Nicola Cásaglì
Yueping Yin · Kyoji Sassa *Editors*

Advancing Culture of Living with Landslides

Volume 4
Diversity of Landslide Forms



A Programme of
the ICL for ISDR

4thWLF₂₀₁₇
4th World Landslide Forum
LJUBLJANA SLOVENIA EU

Springer

Advancing Culture of Living with Landslides

Matjaž Mikoš · Nicola Casagli
Yueping Yin · Kyoji Sassa
Editors

Advancing Culture of Living with Landslides

Volume 4 Diversity of Landslide Forms



Springer

Editors
Matjaž Mikoš
Faculty of Civil and Geodetic Engineering
University of Ljubljana
Ljubljana
Slovenia

Nicola Casagli
Department of Earth Sciences
University of Florence
Florence
Italy

Yueping Yin
China Institute of Geo-Environment Monitoring
China Geological Survey
Beijing
China

Kyoji Sassa
International Consortium on Landslides
Kyoto
Japan

Associate editors
Kazuo Konagai
Department of Urban Innovation
Yokohama National University
Yokohama
Japan

Giovanni Battista Crosta
Department of Earth and Environmental Sciences
Università degli Studi di Milano-Bicocca
Milan
Italy

Hiroshi Fukuoka
Research Institute for Natural Hazards and
Disaster Recovery
Niigata University
Niigata
Japan

Peter Bobrowsky
Geological Survey of Canada
Vancouver
Canada

ISBN 978-3-319-53484-8 ISBN 978-3-319-53485-5 (eBook)
DOI 10.1007/978-3-319-53485-5

Library of Congress Control Number: 2017939909

© Springer International Publishing AG 2017

This work is subject to copyright. All rights are reserved by the Publisher, whether the whole or part of the material is concerned, specifically the rights of translation, reprinting, reuse of illustrations, recitation, broadcasting, reproduction on microfilms or in any other physical way, and transmission or information storage and retrieval, electronic adaptation, computer software, or by similar or dissimilar methodology now known or hereafter developed.

The use of general descriptive names, registered names, trademarks, service marks, etc. in this publication does not imply, even in the absence of a specific statement, that such names are exempt from the relevant protective laws and regulations and therefore free for general use.

The publisher, the authors and the editors are safe to assume that the advice and information in this book are believed to be true and accurate at the date of publication. Neither the publisher nor the authors or the editors give a warranty, express or implied, with respect to the material contained herein or for any errors or omissions that may have been made. The publisher remains neutral with regard to jurisdictional claims in published maps and institutional affiliations.

Hiroshima landslide disasters in August 2014, Hiroshima, Japan (PASCO Corporation—Kokusai Kogyo Co., Ltd. All Rights Reserved)

Printed on acid-free paper

This Springer imprint is published by Springer Nature
The registered company is Springer International Publishing AG
The registered company address is: Gewerbestrasse 11, 6330 Cham, Switzerland

Flash Floods in the Rwenzori Mountains— Focus on the May 2013 Multi-Hazard Kilembe Event

Liesbet Jacobs, Jan Maes, Kewan Mertens, John Sekajugo,
Wim Thiery, Nicole van Lipzig, Jean Poesen, Matthieu Kervyn,
and Olivier Dewitte

Abstract

Over the past 50 years, at least seven major flash floods have affected catchments of the Rwenzori Mountains. The Rwenzori Mountains are not only subject to flash floods; forest fires, earthquakes and landslides occur as well. Many of the flash floods therefore co-occurred with other hazards. One of the most devastating of these events occurred on May 1st 2013, in the Nyamwamba catchment. Here we reconstruct the circumstances under which this flash flood event was triggered and its effects in this multi-hazard region. This includes the identification and characterization of different processes acting upon the catchment dynamics, their controlling and triggering factors and the estimation of the damaging effects of the flash flood within the catchment. The combined occurrence of intense rainfall, a forest fire having burned 18% of the catchment area and the occurrence of 29 landslides providing debris to the river system, induced a debris-rich and very destructive flash flood which caused several fatalities, the destruction of 70 buildings, several bridges, a hospital and a school, a tarmac road and several life lines. Peak flow discharge is estimated between 850 and 1300 m³/s. This case-study demonstrates that flash floods in the region should not be considered as self-determined phenomena but as a result of several cascading and interacting hazard processes including wildfires and landslides, occurring within a short time period.

Keywords

Flash flood • Landslide • Forest fire • Multi-hazard • Equatorial africa

L. Jacobs (✉) · O. Dewitte

Department of Earth Sciences, Royal Museum for Central Africa,
Leuvensesteenweg 13, 3080 Tervuren, Belgium
e-mail: liesbet.jacobs@africamuseum.be

L. Jacobs · J. Maes · M. Kervyn

Department of Geography, Earth System Science, Vrije
Universiteit Brussel, Pleinlaan 2, 1050 Brussels, Belgium

J. Maes · N. van Lipzig · J. Poesen

Division of Geography and Tourism, KU Leuven, Celestijnenlaan
200E, 3001 Heverlee, Belgium

K. Mertens

Division of Bio-Economics, KU Leuven, Celestijnenlaan 200E,
3001 Heverlee, Belgium

J. Sekajugo

Department of Natural Resource Economics, Busitema University,
Kampala, Uganda

W. Thiery

Institute for Atmospheric and Climate Science, Land-Climate
Dynamics, ETH Zürich, Universitätstrasse 16, 8092 Zurich,
Switzerland

W. Thiery

Department of Hydrology and Hydraulic Engineering, Vrije
Universiteit Brussel, Pleinlaan 2, 1050 Brussels, Belgium

Introduction

Flash floods represent an interesting case of multi-hazards as they often result from interactions with forest fires or landslides. Although in recent years a lot of progress was made in quantifying feedback mechanisms and interactions between hazards, large datasets are often required. In the African context, the required intense monitoring of environmental systems and data collection is particularly challenging, due to financial or political constraints and the physically remote character of its mountainous regions.

Western Uganda, and the East African Rift in general, simultaneously appears as a hotspot on global maps for seismic, landslide and cyclone hazards (Hong and Adler 2008; PreventionWeb 2009). The lacuna in even the basic documentation of hazardous events however remains large. This is also the case for the Rwenzori Mountains. This latter region was affected by flash floods at least seven times over the past 50 years. The events often occurred together with or following major earthquakes or landslides. In comparison to the latter, flash floods on average cause more fatalities per

event and each typically displace dozens to hundreds of households (Jacobs et al. 2016a).

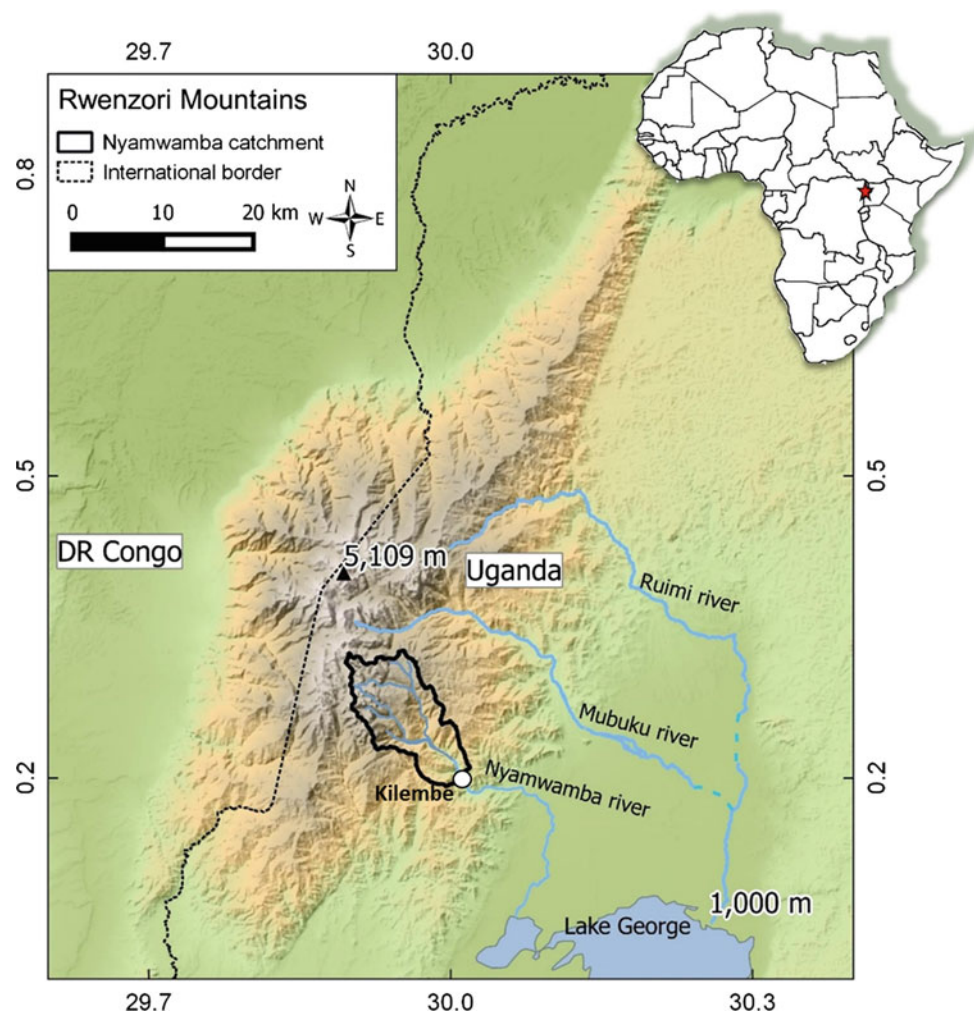
The aim of this study is to increase our understanding of flash flood events in these data-poor and high energy relief areas, using a case study from the Rwenzori Mountains where hazard interactions are expected. For this particular case-study, the occurrence of a large fire further complicates the spectrum of potential hazard interactions. With this study we aim to use a combination of well-established methods of different disciplines to better document and understand these multi-hazards in regions with low accessibility.

Study Region

Regional Setting: The Rwenzori Mountains

The Rwenzori Mountains lie on the border of DR Congo and Uganda. They cover an area of ca. 3000 km² and reach an altitude of 5109 m a.s.l. (Fig. 1). Intense rainfall, high seismic activity and landslides (Jacobs et al. 2016a, b) affect

Fig. 1 location of the Rwenzori Mountains and the Nyamwamba river catchment (Jacobs et al. 2016c)



the region. A full description of the horst mountain's topography, lithology, soils, climate and seismic activity can be found in Jacobs et al. (2016a).

Nyamwamba Catchment and the Town of Kilembe

The town of Kilembe (30.01°E – 0.20°N , Fig. 1) is located in the Nyamwamba catchment. In Kilembe, the catchment covers 107 km^2 and hosts the Nyamwamba river. The lithology consists of gneiss, mica schist with quartzite interbeds and moraine deposits (Fig. 2a; GTK Consortium 2012). Slope gradients regularly exceed the local and global thresholds for slope stability (Jacobs et al. 2016a; Fig. 2b). The catchment is strictly subdivided by a park boundary at 1700 m a.s.l (Fig. 2c). Below this boundary, agriculture and built-up areas are the major land uses. Above 1700 m a.s.l. the national park starts with a dense forest belt up to 2400 m. Above the forest belt, a bamboo belt extends up to 3000 m a.s.l. where the heather forest and shrub zone starts (Eggermont et al. 2009). At the highest elevations in the catchment, rock outcrops and bog land prevails (Fig. 2c). Permanent glaciers are present on the Rwenzori peaks, but the Nyamwamba catchment does not drain the glacier area.

On May 1st 2013, Kilembe was affected by a fatal flash flood. According to an online report of NTV Uganda (2013), the flood started in the afternoon, and river flow was already

strongly reduced (but still above normal) on the 2nd of May. A local NGO reports that the flood occurred around 2 p.m., destroying several bridges after intense rainfall which started at 8 a. m. (LIDEFO 2013). Based on these reports, the flash flood was characterized by a rapid onset with very high initial discharges and a relative short duration. An event of this magnitude was unprecedented in recent years, with an event of similar magnitude observed on April 7th 1966 (Binego 2014 and personal communication with local stakeholders). Most reports on the 2013 event mention intense rainfalls but other potential factors such as mountainous forest fire and landslides in the upper Rwenzori are also reported to potentially have played a role (Binego 2014). In February 2012, the upper part of the catchment was indeed burned. This fire was reported by the Rwenzori Trekking Service and at the time of the fire all touristic activities were suspended and the Kilembe trail was evacuated. The extent of the fire was never mapped. Landslides have also occasionally been reported in the catchment over the past decades, but no spatially explicit inventories have ever been produced for this catchment.

Methods

The Nyamwamba river is not monitored for runoff discharge or sediment transport and no systematic investigation was carried out before, during or directly after the event. The

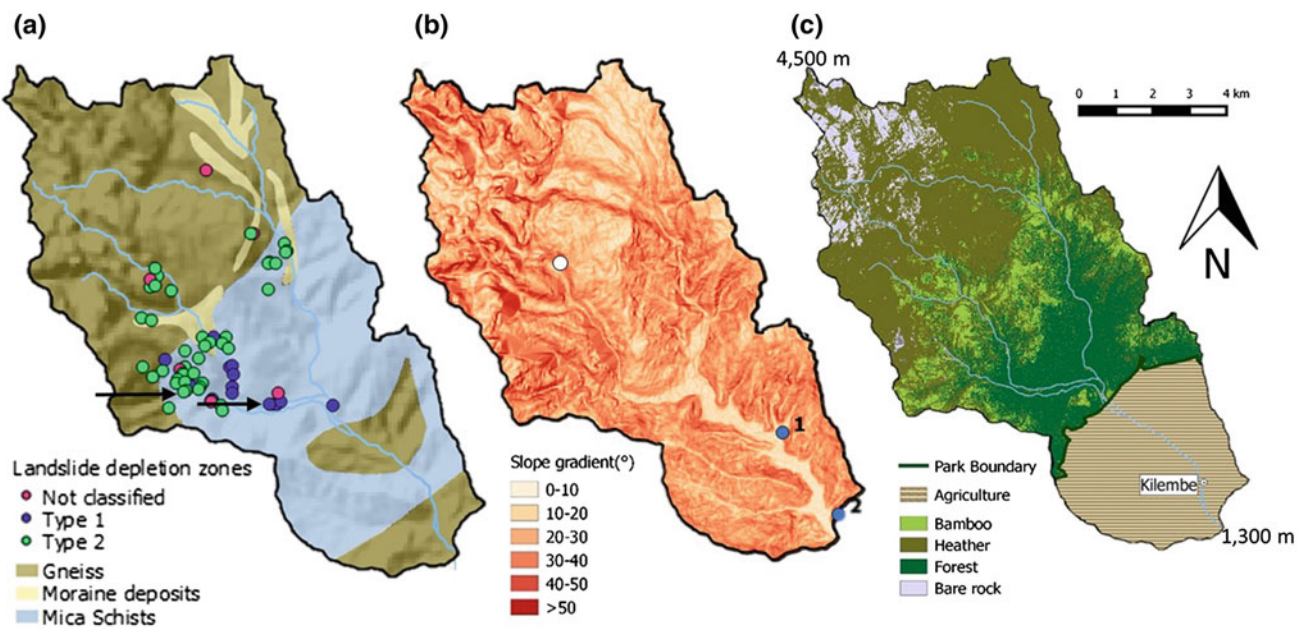


Fig. 2 Biophysical properties of the Nyamwamba catchment. **a** catchment lithology (Source GTK Consortium 2012); location of all identified landslides are indicated by dots **b** catchment slopes derived from SRTM 1" at 30-m resolution (USGS 2014); white dot represents Kalalama camp rainfall station, blue dots represent cross sections

selected for discharge estimation, **c** land cover map derived from supervised classification of the SPOT 6 image shown in Fig. 4. Black arrows show the location of the illustrated landslides in Fig. 5a, b (Jacobs et al. 2016c)

methodology used here is therefore not based on high-input models or extensive field monitoring data but instead includes a combination of remote sensing, exploratory post-disaster field work and field reports by disaster relief organizations, specifically suited for non-accessible, data-poor, multi-hazard environments.

Reconstruction of the Triggering Rainfall Event

For the period preceding the flood, rainfall data (temporal resolution of 24 h) from two rain gauges in the catchment were made available by Africa Nyamwamba Ltd (personal communication). The rain gauges are located in the upper catchment at 3140 m a.s.l. (Kalalama camp, Fig. 2b) and in Kilembe town (1500 m a.s.l.). Data from four rain gauges located in the adjacent catchment to the north of the Nyamwamba catchment were made available by the Uganda Wildlife Authority (UWA). A regional climate model output on a $7 \times 7 \text{ km}^2$ resolution between 1999 and 2008 presented by Thiery et al. (2015) is used to estimate the recurrence interval of the triggering rainfall event.

Reconstruction of the Peak Flow Discharges

For the reconstruction of the peak flow discharges of the Nyamwamba river, Manning's equation Eq. (1) was applied to two river cross sections (Figs. 2b and 3).

$$Q = 1/n * A * R^{(2/3)} S^{0.5} \quad (1)$$

With Q the river discharge, A the river cross section, R the hydraulic radius, n the Manning roughness coefficient and S the water surface slope. For the first cross section, measurements of the river cross section and local slope were

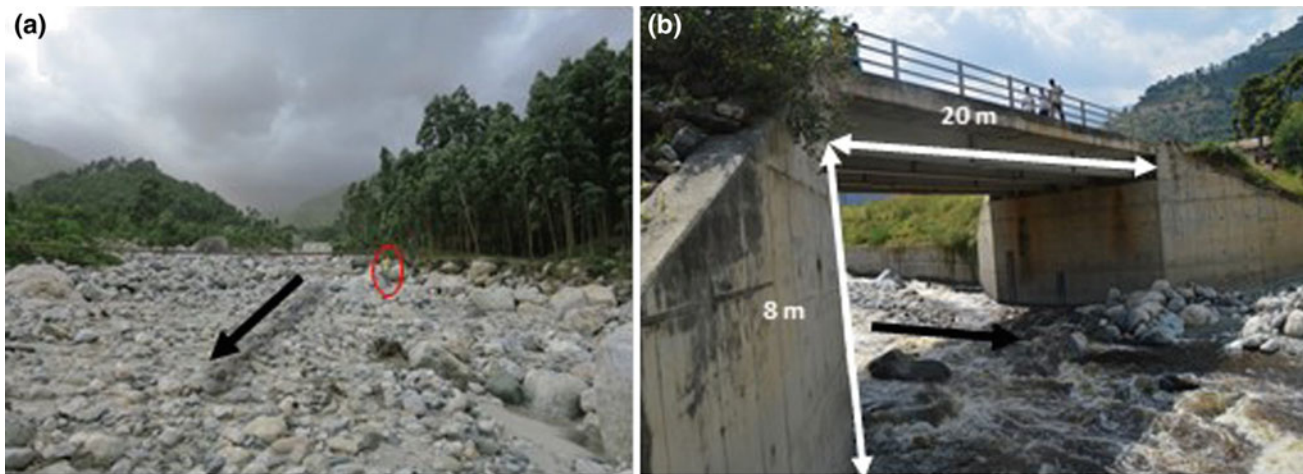


Fig. 3 River cross-sections selected for peak flow discharge estimations

made and the roughness of the river bed was described in the field (Fig. 3a). As a second cross section, a bridge was selected downstream of the first cross section (Fig. 3b) where the water reached the level of the tarmac road. Here the local slope was estimated using a 1:50,000 topographic map (Department of Lands and Survey Uganda 1972). The bridge itself is not supported by piers and during peak discharge the water level reached the tarmac of the bridge (Fig. 3b).

Manning's roughness coefficients were estimated by using descriptive data by Barnes (1967) and tables by Chow (1959) and by the empirical equation for mountain rivers by Jarret (1989):

$$n = 0.32 * S^{0.38} * R^{-0.16} \quad (2)$$

To reduce uncertainty, the estimated discharges were first compared to the global maximum possible discharges (Q_p) with regard to catchment size (C) (Lumbroso and Gaume 2012):

$$\begin{aligned} Q_p &= 500 * C^{0.43} \text{ for } C > 100 \text{ km}^2 \\ \text{or } Q_p &= 100 * C^{0.8} \text{ for } C < 100 \text{ km}^2 \end{aligned} \quad (3)$$

As a second check, the flow velocities (v) and Froude-number (Fr) were calculated using the following equation with g the acceleration due to gravity (m/s^2) and d the mean flow depth (m) (Lumbroso and Gaume 2012):

$$Fr = v/(d * g)^{0.5} \quad (4)$$

Manning's equation as applied here holds for open natural channels. The bridge at the second cross section was however overflowed with water at peak discharge. Therefore a pressure flow regime is more likely (Brunner and Hunt 1995). In the fully submerged scenario, the flow within the cross section of the bridge, can be calculated using following equation:

$$Q_{pr} = C_1 * A * (2 * g * H_1)^{0.5} \quad (5)$$

With C_1 the discharge coefficient (typically 0.8), A the cross section (m^2) and H_1 the elevation difference between upstream and downstream energy gradelines (m) (Brunner and Hunt 1995). Footage taken a day after the flood shows that a rough estimation of the H_1 -value at max. 2 m (± 0.5 m) is reasonable (Kizito 2013). For the total peak flow discharge, also the flow overtopping the bridge should be taken into account but in this case, this is negligible compared to Q_{pr} (Jacobs et al. 2016c). Equations 3, 4 and 5 serve as a constraint to the estimated peak flow discharges using Manning's approach.

Reconstruction of the Factors Potentially Increasing the Flood Magnitude

1. Fire reconstruction

To identify the timing and extent of the fire, the MOD-VOLC algorithm was used (Wright et al. 2004) through the online application of the University of Hawai'i (2004). Details on the method can be found in Jacobs et al. (2016c).

2. Landslide identification

To identify the landslides occurring at the time of the flood, a combination of Google Earth (GE) images (Google Earth 2014a), SPOT 6 images and field observations are used. The use of GE post-event Digital Globe images (February 2014, spatial resolution <1 m) allows the identification of recent landslides. A field survey in September 2014 serves as a validation of the landslides indicated on the GE images. A comparison of these results with a pre-event SPOT 6 image acquired in January 2013 (1.5 m resolution, pan-sharpened) enables the identification of landslides that occurred after January 2013 or that were reactivated between January 2013 and February 2014. These slides are considered to have occurred during the rainfall event of May 1st 2013 (for details, we refer to Jacobs et al. 2016c).

Table 1 Cross-section characteristics and estimated peak-discharges, flow velocities and Froude numbers

Parameter	Discharge point 1 ($C = 84.7 \text{ km}^2$)				Discharge point 2 ($C = 107 \text{ km}^2$)			
		$Q (\text{m}^3/\text{s})$	$V (\text{m/s})$	Fr		$Q (\text{m}^3/\text{s})$	$V (\text{m/s})$	Fr
$A (\text{m}^2)$	190				181			
$P (\text{m})$	79				35.5			
$R (\text{m})$	2.40				5.09			
$S (\text{m/m})$	0.06				0.045			
$D (\text{m})$	2.48				8.68			
n-estimate	0.06	1387	7.3	1.5	0.06	1891	10.5	1.1
	0.075	1110	5.8	1.2	0.075	1513	8.4	0.9
Jarret's n	0.098	849	4.5	0.9	0.088	1290	7.1	0.8

Estimating Damage Caused by the Flash Flood

By using pre and post-event satellite imagery (Google Earth 2010, 2014b), externally available reports and field observations, a damage inventory for this flood was assembled Jacobs et al. (2016c).

Results

Rainfall Conditions Triggering the Flood

On May 1st 2013, 180.6 mm of rainfall was measured at Kalalama camp (Fig. 2b) and 98.3 mm in Kilembe. The days preceding the event were characterized by moderate to low rainfall amounts. Based on the high-resolution regional climate model results by Thiery et al. (2015), the 24 h precipitation limit of 180.6 mm was exceeded four times at Kalalama camp between 1999 and 2008 and its estimated return period is 2.9 years. From reports on this flash flood (LIDEFO 2013; Reliefweb 2013), the 98 mm rainfall observed on May 1st in Kilembe town was concentrated in ca. 6–8 h. The return periods for this rainfall observed over 6–8 h was calculated and found to range from 6.6 to 5.3 years respectively.

Peak Flow Discharge Estimations

Summary data and the Manning's discharge estimated at the two cross sections are shown in Table 1. The peak flow discharge estimates vary from ca. 850 m^3/s —ca. 1900 m^3/s and depend strongly on the applied Manning's coefficient. All the estimated discharges fall far below the envelope maximum discharge of ca. 3800 and 3500 m^3/s for catchments of 84.7 and 107 km^2 respectively, calculated using Eq. 3. The pressure peak flow discharge calculated using Eq. (5) is estimated to be 910 m^3/s ($\pm 13\%$) for the second cross section.

Fire

A fire was detected on MODIS images between the 9th and 11th of February 2012 and covered an area of 42 km² (Fig. 4). The delineated fire corresponds well to the occurrence of bare rock visible on the SPOT6 image taken in January 2013, i.e. almost one year after the fire (Fig. 4). This bare rock was also observed in the field in September 2014. A total burned area of 19 km² was located within the Nyamwamba catchment, accounting for 18% of its surface area at the second cross section. A total cumulative rainfall of <0.2 mm was measured in the four weeks preceding the fire (Jacobs et al. 2016c).

Landslides

Two categories of landslides are distinguished: (1) landslides adjacent to the river with lengths typically equal or smaller than twice the maximal width, hereafter referred to as Type 1 (Fig. 5) and (2) debris flows or slides with typically a narrow run-out zone, not necessarily connected to the river system (length typically larger than three times the maximal width, Type 2; Fig. 5). Based on field observations of deep scour

and the typically wide base of the Type 1 landslides, they are interpreted to have been triggered by scour and bank failure at the slide foot. Type 2 landslides are triggered directly by rainfall. This distinction is relevant because of their different triggering mechanism and their different role in the hazard interactions. Generally we consider that Type 2 landslides are triggered at their top, while the Type 1 landslides are triggered close to their base.

In total, 67 landslides are identified, covering an area of 207 × 10³ m². On May 1st 2013 50 slides were activated and 5 slides reactivated. Of these slides, 15 landslides belong to Type 1 slides. All except 1 of this type of landslide were triggered on May 1st 2013 by high river discharge. These Type 1 slides account for 58% of the surface of landslide bodies that are candidates for debris supply to the river on the 1st of May 2013. The remaining slides consist of 34 Type 2 slides and six unclassified slides. No evidence of river damming was observed in the field, however a systematic survey of the river channel was not possible due to its poor accessibility. Therefore (partial) landslide damming cannot be ruled out with certainty.

Based on the lithological map (GTK Consortium 2012), landslides are mainly concentrated on the mica schists and moraine deposits (70 and 18% of the landslides respectively)

Fig. 4 Extent of the fire overlain on the SPOT6 pan-sharpened image acquired in January 2013

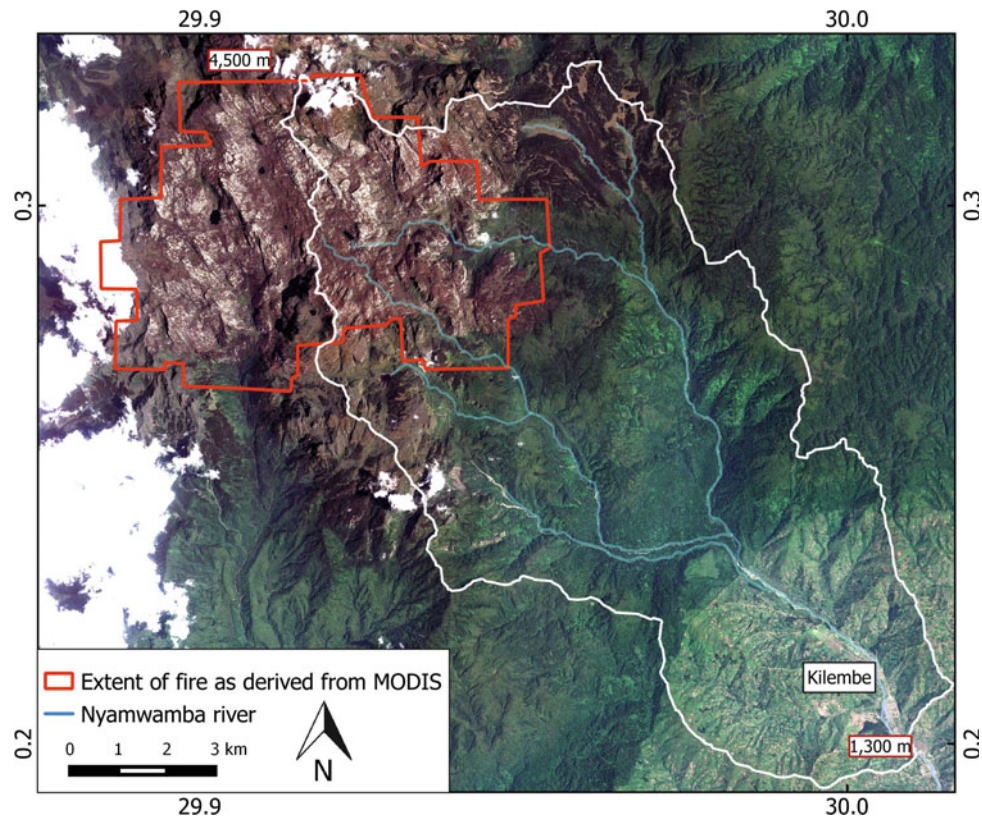




Fig. 5 Illustration of the two landslide types. **a, c** landslides adjacent to the river with large width-to-length ratios. **b, d** debris flows with a narrow run-out zone. *Top* landslides observed with GE images and

bottom examples observed in the field do not depict the same landslides, but serve as illustration

even though gneiss is the dominant lithology in the catchment (55% of the catchment). When analyzing the distribution of slope angles of the catchment in comparison to the distribution of slopes where the landslides occur, a concentration of slides on the steeper slopes can be observed with 60% of the landslides occurring on slopes greater than 30°.

Damage Estimations

The damage inventories are given in Table 2. The buildings destroyed or damaged show both signs of water damage as well as damage through the impact of large boulders (Fig. 6a–c). These transported boulders have a diameter

Table 2 Damage inventory summary. Reports used: ActAlliance (2013), Reliefweb (2013). GE = Google Earth FW = Field Work

Type	Reported damage	GE	FW
Fatalities	6–8	N/A	N/A
Community infra-structure	Kilembe Hospital partially destroyed, staff quarters entirely destroyed, Bulemba primary school entirely destroyed	N/A	N/A
Lifelines	2 pipelines and several drinking wells destroyed, hydro power station blacked-out	N/A	N/A
Housing infra-structure	70 buildings destroyed	57 buildings destroyed	66 buildings destroyed, 9 damaged
Road infra-structure	5 bridges washed away	3 bridges and 470 m of tarmac road destroyed	N/A

**Fig. 6** Examples of damage caused by the flood. **a** River bed and scour, **b** destruction of house foundation (white arrow), **c** destruction of house due to impact from debris (black arrow), **d** illustration of boulder size frequently found in the valley (backpack for scale)

exceeding 1.5 m (Fig. 6d). The foundation of the buildings nearest to the river bed were often completely destroyed (Fig. 6b). Furthermore, the damage to infrastructure and specifically buildings, tarmac roads and bridges can only be explained by the large volume of debris transported by this high-energy torrent. The increase in area covered by debris in the Nyamwamba valley up to Kasese town is 34.4%.

Discussion

Reconstruction of the May 2013 Event

The rainfall depth in the upper catchment was exceeded four times in the past 10 years and therefore not unusual. However in the past decades, no flash floods of similar magnitude were reported in this catchment (Jacobs et al. 2016c).

This indicates that the observed heavy precipitation cannot be considered to be the only factor causing this flash flood.

Using several cross-checking approaches (see details in Jacobs et al. 2016c), peak flow discharges ranging between ca. 850 m³/s at the first cross section (based on the Manning's peak flow discharge estimation) and 910 m³/s (based on the pressure discharge calculation) at the second cross section are identified to be the most realistic. The velocities associated with these discharges range from 4.5 to 5 m/s, which is a good indication for debris transport (Lumbroso and Gaume 2012). These discharge estimations are almost two orders of magnitude larger than the mean daily historic discharge measured on two neighbor rivers with the same climatic and topographic conditions as river Nyamwamba (Jacobs et al. 2016c).

Increase in peak discharges is generally considered to be a primary response after a wildfire (Moody and Martin 2001). Indeed, the order of magnitude and exceptionality of this peak flow discharge does not correspond to the relatively frequent recurrence of the triggering rainfall depth indicating the need to consider the effects of the fire and landslides.

The landslides (re)activated on May 1st 2013 also aggravated the nature of the flood by supplying debris to the river flow. Some of the landslides are furthermore indirectly triggered by the fire. Although none of the landslides occurred in the burned area, more than half of the debris-supplying landslides are triggered at least partially by an increased river flow which for this flood event, as stated above, can mainly be explained due to the fire. This illustrates the importance of distinguishing between the two types of landslides. All these interactions need to be taken into account to fully understand the potential hazard interactions and cascades.

The spatial distribution of landslides is strongly connected to the occurrence of moraine deposits and mica schists and on slope angles above 35°. Catchments in the Rwenzori Mountains with similar topography and lithology are expected to be particularly hazardous for floods by supplying debris to the river system.

The reconstruction of damage using satellite images provides realistic estimates of the number of buildings and their concentration in space. Limited field work is advised to have an idea about the importance of debris transport in the damage patterns.

Probability of Future Flash Flood Events

With an estimated return period of maximum 6.6 years, the rainfall event of May 1st 2013 is not exceptional. However

the flash flood triggered by this event does not have the same frequency, indicating the importance of assessing the probability of other phenomena like fire or landslides to assess the potential for similar flood events.

Although the February 2012 fire was unique in terms of size and elevation over the last 15 years, traces of previous fire in the Rwenzori Mountains were found by Wesche et al. (2000). Because it is projected with medium confidence that periods of drought will intensify in East-Africa under anthropogenic climate change (Niang et al. 2014), the likelihood of long periods of drought preconditioning fires is expected to increase as well. Considering that fires may also be induced by human activity in the Rwenzori, an increased human presence due to poaching or tourism could also increase the frequency of fire triggers.

The role of landslides in aggravating flash flood can also be linked to the last major flash flood of comparable magnitude which occurred in the catchment on April 7th 1966 (Binego 2014). A series of large seismic shocks starting from March 20th 1966 ($M = 6.1$) (UNESCO 1966) triggered landslides throughout the Rwenzori Mountain range. These last two major flash floods in the catchment show that the role of landslides in the propagation of flash floods cannot be neglected and their probability should be assessed and taken into account when considering flash flood hazard. Finally, with a projected increase in heavy precipitation events, the frequency of rainfall-triggered landslides and flash floods is likely to increase (Niang et al. 2014).

Conclusions

The Kilembe case study shows that even a rainfall event with a relatively short return period can cause a disastrous flash flood event. This peak discharge can only be explained through the complex response of the catchment to the occurrence of fires and landslides (Fig. 7). This study demonstrates the need to consider flash floods as a combination of multiple hazards and not as self-determined phenomena for disaster risk reduction.

The methodologies used in this study do not require detailed field work nor intensive system monitoring and can as such be applied to other similar multi-hazard environments with low data availability. This approach is needed to quickly develop and reinforce correct legislations and to take appropriate actions when a fire, a storm, or an earthquake occurs, taking into account all possible current and future multi-hazard interactions.

Acknowledgements We thank the VLIR UOS South Initiative project (ZEIN2013Z145) and the BELSPO AfReSlide project (BR/121/A2/AfReSlide) for financial support. Special acknowledgements go to

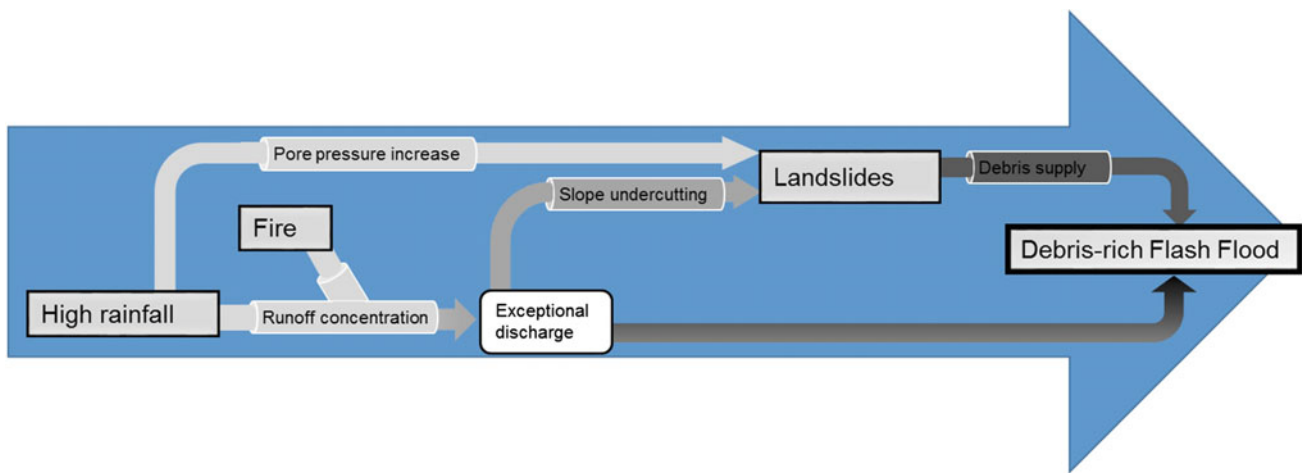


Fig. 7 Hazards (black squares), cascade effects, interactions and processes at play during the Kilembe flood on May 1st 2013 (Jacobs et al. 2016c)

the Kilembe Trekking Service, the Uganda Wildlife Authority, the Africa Nyamwamba Ltd, the Kasese district authorities and the Kilembe authorities, Mountains of the Moon University and all organizations and persons providing background reports and documenting the flood.

References

- ActAlliance (2013) Preliminary appeal UGANDA flash floods in Kasese—UGA131. http://reliefweb.int/sites/reliefweb.int/files/resources/UGA131Prel_KaseseFL.pdf. Accessed 22 Apr 2015
- Barnes H (1967) Roughness characteristics of natural channels. USGS surv watter-supply, p 219
- Binego A (2014) Causes of river Nyamwamba floods. <http://www.newvision.co.ug/mobile/Detail.aspx?NewsID=651297&CatID=4>. Accessed 15 Apr 2015
- Brunner and Hunt (1995) A comparison of the One-dimensional bridge hydraulic routines from: HEC-RAS, HEC-2 and WSPRO. US army corps of engineers, hydrologic engineering center. <http://www.hec.usace.army.mil/publications/ResearchDocuments/RD-41.pdf>. Accessed 14 June 2016
- Chow V (1959) Open-channel hydraulics. McGraw-Hill Book Co., New York
- Department of Lands and Survey Uganda (1972) Topographic map of Kasese sheet 66/3(1):50,000
- Eggermont H, Van Damme K, Russell JM (2009) Rwenzori mountains (mountains of the moon): headwaters of the white nile. In: Dumont HJ (ed) Nile Orig. Environ. Limnol. Hum. use. Springer, Netherlands, pp 243–261
- Google Earth (2010) Nyamwamba valley february 15 2014, 0.25°N, 30°E, digital globe 2015. <http://www.earth.google.com>. Accessed 4 Apr 2015
- Google Earth (2014a) Nyamwamba valley february 15 2014, 0.25°N, 30°E, digital globe 2015. <http://www.earth.google.com>. Accessed 4 Apr 2015
- Google Earth (2014b) Nyamwamba valley january 13 2014, 0.25°N, 30°E, digital globe 2015. <http://www.earth.google.com>. 4 Apr 2015
- GTK Consortium (2012) Geological map of Uganda 1:100,000 Sheet N 65 Karambi
- Hong Y, Adler R (2008) Predicting global landslide spatiotemporal distribution: integrating landslide susceptibility zoning techniques and real-time satellite rainfall estimates. Int J Sed Res 23:249–257. doi:[10.1016/S1001-6279\(08\)60022-0](https://doi.org/10.1016/S1001-6279(08)60022-0)
- Jacobs L, Dewitte O, Poesen J, Delvaux D, Thiery W, Kervyn M (2016a) The Rwenzori mountains, a landslide-prone region? Landslides. doi:[10.1007/s10346-015-0582-5](https://doi.org/10.1007/s10346-015-0582-5)
- Jacobs L, Dewitte O, Poesen J, Maes J, Mertens K, Sekajugo J, Kervyn M (2016b) Landslide characteristics and spatial distribution in the Rwenzori mountains, Uganda. J African Earth Sci. doi:[10.1016/j.jafrearsci.2016.05.013](https://doi.org/10.1016/j.jafrearsci.2016.05.013)
- Jacobs L, Maes J, Mertens K, Sekajugo J, Thiery W, van Lipzig N, Poesen J, Kervyn M, Dewitte O (2016c) Reconstruction of a flash flood event through a multi-hazard approach: focus on the Rwenzori mountains, Uganda. Nat Hazards. doi:[10.1007/s11069-016-2458-y](https://doi.org/10.1007/s11069-016-2458-y)
- Jarrett RD (1989) Hydrologic and hydraulic research in mountain rivers. IAHS-AISH Publ 190:107–117
- Kizito BJ (2013) Kilembe floods. <https://www.youtube.com/watch?v=4jTSBGRznBM>. Accessed 16 Apr 2015
- LIDEFO (2013) Lidefo News-Kasese floods. <http://lidefo-uganda.blogspot.co.at/2013/05/v-behaviorldefaultvml.html>. Accessed 22 Apr 2015
- Lumbroso D, Gaume E (2012) Reducing the uncertainty in indirect estimates of extreme flash flood discharges. J Hydrol 414–415:16–30. doi:[10.1016/j.jhydrol.2011.08.048](https://doi.org/10.1016/j.jhydrol.2011.08.048)
- Moody JA, Martin DA (2001) Post-fire, rainfall intensity-peak discharge relations for three mountainous watersheds in the Western USA. Hydrol Process 15:2981–2993. doi:[10.1002/hyp.386](https://doi.org/10.1002/hyp.386)
- Niang I, Ruppel OC, Abdrabo MA et al (2014) Africa. In: Climate change 2014: impacts, adaptation, and vulnerability. Part B: regional aspects. Cambridge University Press, Cambridge, pp 1199–1265
- NTV Uganda (2013) Online video report: Kasese Floods situation. <https://www.youtube.com/watch?v=kANu7O82iSM>. Accessed 15 Mar 2015
- PreventionWeb (2009) Global distribution of multiple hazards mortality risk. <http://preventionweb.net/go/10605>. Accessed 8 Dec 2015
- Reliefweb (2013) Disaster relief emergency fund (DREF) Uganda: Kasese floods http://reliefweb.int/sites/reliefweb.int/files/resources/Uganda_Kasese_Floods_DREF_operation_MDRUG033.pdf. Accessed 4 May 2015

- Thiery W, Davin E, Panits H-J et al (2015) The impact of the African great lakes on the regional climate. *J Clim* 28:4061–4085. doi:[10.1175/JCLI-D-14-00565.1](https://doi.org/10.1175/JCLI-D-14-00565.1)
- UNESCO (1966) Earthquake reconnaissance mission, Uganda, the toro earthquake of 20 March 1966. <http://unesdoc.unesco.org/images/0000/000077/007799EB.pdf>. Accessed 1 May 2015
- University of Hawai'i (2004) MODVOLC Near-real-time thermal monitoring of global hot-spots. modis.higp.hawaii.edu. Accessed 10 Feb 2015
- USGS (2014) Shuttle radar topography mission, 1 arc second scenes SRTM1N00E030V3, SRTM1N00E029V3, SRTM1S01E030V3, SRTM1S01E029V3. Unfilled Unfinished, Global Land Cover Facility, University of Maryland, College Park, Maryland February 2000
- Wesche K, Miehe G, Kaeppli M (2000) The significance of fire for afroalpine ericaceous vegetation. *Mt Res Dev* 20:340–347. doi:[10.1659/0276-4741\(2000\)020\[0340:TSOFFA\]2.0.CO;2](https://doi.org/10.1659/0276-4741(2000)020[0340:TSOFFA]2.0.CO;2)
- Wright R, Flynn LP, Garbeil H et al (2004) MODVOLC: Near-real-time thermal monitoring of global volcanism. *J Volcanol Geotherm Res* 135:29–49. doi:[10.1016/j.jvolgeores.2003.12.008](https://doi.org/10.1016/j.jvolgeores.2003.12.008)